GEOLOGICA CARPATHICA, JUNE 2023, 74, 3, 261–277 https://doi.org/10.31577/GeolCarp.2023.11

Tectonic inversion of Late Miocene extensional deformations in northeastern Tunisia (Cap Bon Peninsula–Sahel area)

RAOUF GHRIBI[1,✉], HASSENE AFFOURI[1] and SAMIR BOUAZIZ[2]

[1]Department of Earth Sciences, Faculty of Sciences of Sfax, University of Sfax, B.P. 1171, Sfax 3000, Tunisia; ✉raouf.ghribi@fss.usf.tn
[2]National Engineering School of Sfax, University of Sfax, B.P. W. 3038, Sfax, Tunisia

(Manuscript received January 21, 2022; accepted in revised form April 11, 2023; Associate Editor: Michal Šujan)

Abstract: The tectonic inversion of the Miocene extensional basins (Cap Bon Peninsula–Sahel area, northeastern Tunisia) is an important process that accommodates the crustal shortening in the northeastern Tunisian edge with the ongoing collision between the African and European plates. Field observations and microtectonic measurements have revealed two main Late Miocene tectonic events: (1) A NE–SW trending extensional tectonic event that would create titled blocks, horsts, and grabens, as well as slump features. These structures were controlled by numerous conjugate systems of syndepositional normal faults. On a regional scale, the NW-trending faults controlled the Miocene sedimentation and subsidence rate in the Takelsa, Dakhla, Saouaf, and Zeramdine syn-rift grabens and (2) the NW-directed post-Tortonian compression, the so-called "Alpine/Atlasic event" that was identified by NE–SW-oriented reverse slip movements and associated folds. The latter compressional event began in the latest Miocene and continued through the Plio–Quaternary, which thus led to the complete inversion of the Miocene basins by the ongoing African and European plates' convergence. A significant neotectonic uplift of the Abderrahmane, Korbus, and Skanes areas recorded the switch from Late Miocene crustal extension to post-Tortonian to Quaternary compressional tectonics. In fact, the present-day petroleum trap configuration of the northeastern offshore Tunisia is highly controlled to the Miocene–Quaternary tectonic inversion. The sandy levels along the thick Tortonian section provided the most preferred target for petroleum exploration. They exhibit considerable variations in thickness controlled by Late Miocene to Quaternary tectonic trends.

Keywords: northeastern Tunisia, Late Miocene deformations, Miocene–Quaternary tectonic inversion, petroleum inversion-related traps

Introduction

The concept of structural inversion was used for the first time in the early 1980s (Glennie & Boegner 1981). Several mechanisms have been proposed to explain basin inversion in terms of dip-slip faults motion. Isostatic, flexural, thermal, and tectonic mechanisms drive the compressional reactivation of faults. Many authors have reviewed those mechanisms as occurring in continent–continent or arc–continent collision margins (McClay & Buchanan 1992; Levander et al. 2014; Van Hinsbergen et al. 2014). They are also related to changes in the rate and dip of subduction at ocean-continent convergent margins. However, the most common type refers to the compressional reactivation of the pre-existing normal faults in sedimentary basins and passive margins that originally formed by extension or transtension (Turner & Williams 2004). Fault reactivation may change the architecture of the basin and commonly results in the uplift of previously-subsided areas and the exhumation of formerly buried rocks. The inversion interpretations need to rely on the regional understanding of different stages of the basin evolution, which started with extensional deformations characterized by syn-rift structures. Tectonic inversion is driven by the ongoing horizontal shortening related to plates convergence. The moderate inversion-related folds offered the most preferred drilling targets for hydrocarbon exploration (Cooper et al. 1989; Buchanan & Buchanan 1995). The post-tectonic covers yield a seal for petroleum reservoir.

The Late Miocene to Quaternary tectonic evolution of northeastern Tunisia started with crustal extension. Syn-depositional fault movements created subsiding blocks and controlled the late Miocene siliciclastic sedimentation (Bedir et al. 1996; Azizi & Chihi 2021). As a consequence of the shortening event during the Late Tortonian to Quaternary times, folds and thrust faulting have been generated. They are related to the NW–SE convergence movement between Africa and Eurasia (Ben Ayed et al. 1983; Burollet & Ellouze 1986; Ben Romdhane et al. 2006; Azizi & Chihi 2016). Zouaghi et al. (2011) assigned the formation of drag folds, synclinal basins, and grabens in eastern Tunisia to the Neogene transtensional and transpressional movements of the N to NW-striking system faults without considering the chronology of paleostress. Booth-Rea et al. (2018) argued ENE and SE striking of extensional fault systems in the north of Tunisia were related to the tearing of the Calabrian slab along the Tunisian Atlas during the Late Tortonian to Pliocene times. However, understanding of the Late Neogene to Quaternary evolution of northeastern Tunisia is important for the interpretations of its tectonic inversion. It was therefore necessary to carry out systematic fieldwork to further explain stress chronology and

(cc) BY-NC-ND

fault reactivation. Special attention has been given to the chronology between extensional and compressional events by data examination for all possible superimposed striations on fault planes or crosscutting relationships between faults.

In this paper, we used numerous sets of faults and joints measurements to determine the Late Miocene to Quaternary stress axis trends using the Direct Stress Inversion (INVD) method by Angelier (1991). The field-based paleostress chronology is specified by slickenside intersection of striated fault planes. Paleostress analysis was carried out at seven microtectonic sites in northeastern Tunisia, including the Cap Bon Peninsula, Takelsa, Saouaf, Monastir, Jemmal, Zeramdine, and Ksour Essaf (Mahdia) in order to reconstruct the Late Miocene tectonic trends (Fig. 1). Furthermore, we use available reflexion seismic profiles and isopach maps to understand the post-Tortonian to Quaternary tectonic inversion of pre-existing syn-rift structures. The inverted geometry generated Miocene petroleum traps known offshore of Hammamet by wells correlation.

Geological setting

The most distinctive tectonic feature of the Cap Bon Peninsula is the Abderrahmane belt, which is a northern extension block of the Zaghouan fold-thrust belt. Further to the south, NE–SW-trending segments of the foreland basins of Dakhla and Takelsa roughly parallel the deformational front of the Abderrahmane anticline. The onshore relay-zone of the Cap Bon Peninsula with the Siculo–Tunisian Strait is the Sidi Daoud graben. The north and northwest-trending faults controlled the network drainage of the Cap Bon Peninsula and bounded the margins of the Bouficha and Grombalia grabens. The Zaghouan thrust fault outlines the northern margin of the gentle topography of the Sahel area. The northern part of the Tunisian Sahel is underlined by NE-trending "*en echelon*" folds, such as the Enfidha anticline, which is also recognised (Fig. 1). Several fault-controlled basins are characterised by thick series of the Miocene to Quaternary, such as the Zeramdine and Saouaf graben structures. The characteristic Hammamet–Monastir fault strikes NNW–SSE for more than 60 km along the entire margin of the Cap Bon and Monastir peninsulas. Its northern and southern segments exhibited strike-slip movement with normal components. This fault has played an intrinsic role throughout the evolution of northeastern Tunisia, outlining the triangular-shaped Grombalia graben (Ghribi et al. 2018).

Miocene–Quaternary lithostratigraphic description

The Sahel–Cap Bon area was covered dominantly by Oligo–Miocene to Quaternary deposits with various lithology and fauna associations. Their thickness is highly variable from a few meters up to 2500 m. Lithostratigraphic data show interesting unconformities that coincide with the change in the sea level and are related to the synchronous intrabasinal deformations. The Oligo–Miocene series attributed to the Fortuna Formation and are well-developed in Jebel Abderrahmane (700 m), since they are sandy and interbedded with shale and silt (Ben Salem 1992; Hooyberghs 1995). The Langhian interval (Ain Grab Formation) is represented by metric bioclastic limestone beds reaching 45 m in thickness in Korbus, which overlies the Fortuna Formation by thin layers of conglomerates. The described fauna are Echnids, Pectinidae, and Bryozoa, indicating a stratigraphical unconformity corresponding to the biozone N9 (Bismuth & Hooyberghs 1994). The Mahmoud Formation is predominantly composed of marls. The presence of *Orbulina universa* and *Orbulina suturalis* supports an upper Langhian to Serravalian age (Biely et al. 1972; Besème & Blondel 1982; Ben Salem 1992). The Beglia Formation in Serravalian age is formed by sandstone beds with marl intercalations. The thickness of these sediments varies greatly, ranging from 20 m thick at Jebel Abderrahmane to 500 m in the Gulf of Hammamet, where it is replaced by the Birsa Formation (Ben Ferjani et al. 1990; Boujamaoui et al. 2000). Three members (Lower Birsa, Intra-Birsa and Upper Birsa) are recognised from well data, and they are characterized by sandstone bodies with abundant planktonic fauna and interbedded shale and limestone layers (Fares et al. 2006). The Late Miocene deposits referred to as the Saouaf Formation are well-developed in the Zeramdine, Monastir (Sahel area), Saouaf syncline, and Oum douil-Takelsa areas (Cap Bon Peninsula), where numerous quarries and stream cuts have exposed vertical and lateral lithology variations (Fig. 1). In the Jemmal area, the Tortonian series consist of thick sequences of interbedded fossiliferous sandstone and clays that enclose several lignitiferous layers (1100 m). Their described biotas are mostly gastropods, oysters, and forams, such as *Ostrea crassissima*, *Turritelle fimbriata MICH, Cerithium lignitarum EICHW,* and *Globorotalia acostaensis* giving a Tortonian age (Biely et al. 1972; Demarcq et al. 1976; Hooyberghs 1987). In the 2 km fairway of Jemmal city, the Tortonian thickness rapidly increases in the Zeramdine area reaching 2000 m. Along the Skanes–Monastir coastal cliffs, Tortonian layers are predominantly composed of sandstones at the base, becoming more clayey with lignite beds at the top. Its thickness ranges from 950 to 1100 m. They are apparently truncated by an angular unconformity and sealed by Pliocene and Tyrrhenian sediments (Ghribi & Bouaziz 2010). Further north, the Tortonian deposits show gradually increasing thickness within the Takelsa syncline, where more than 2500 m of thickness are reported (Hooyberghs & Ben Salem 1999). A drastic reduction of thickness was observed at the margin of Abderrahmane belt where only 90 m of the Saouaf Formation is present (Ben Ismail-Lattrache 1981; Ben Ferjani et al. 1990). The Tortonian deposits are overlain by fluvio-continental deposits of the Somaa Unit, which outcrops in the southern part of the Cap Bon Peninsula and near the Beni Khiar Formation. They are early Messinian in age and consist of fossiliferous limestone, sand, and clay (Colleuil 1976; Besème & Kamoun 1988; Hooyberghs & Ben Salem 1999; Kamoun et al.

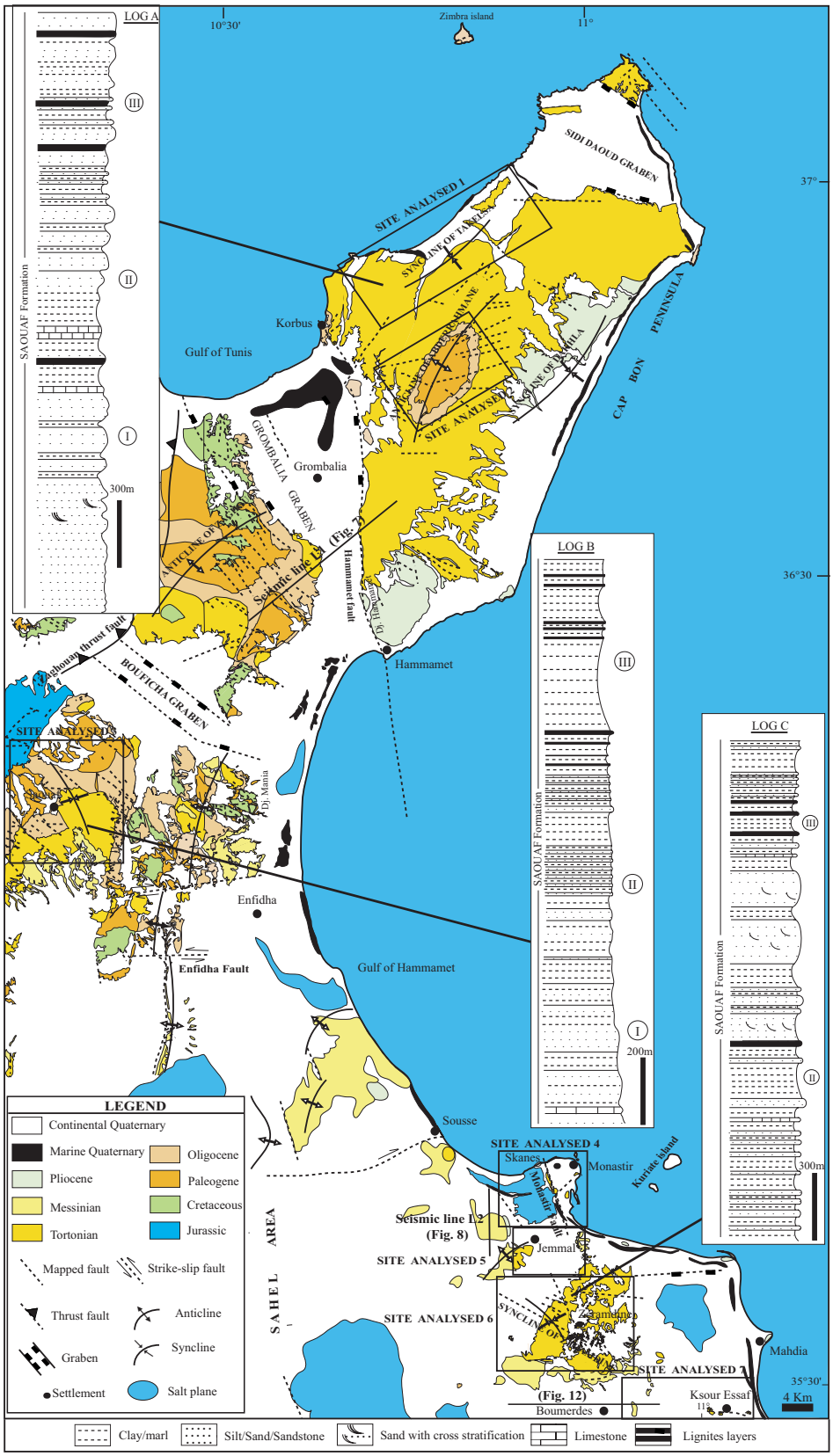

Fig. 1. Geological map of northeastern Tunisia. Tortonian sequences exposed in Takelsa syncline (Log A), in Saouaf syncline (Ben Moktar & Mannaï-Tayech 2012; Log B) and in Zeramdine area (Ghribi & Bouaziz 2010; Log C). Folds and faults were mapped from 1:50,000 detailed geological maps. Boxes indicate tectonic sites discussed in the text. Thick lines represent the locations of the seismic profiles L1 & L2 and cross-section trace.

2001; Gaaloul & Razgallah 2008; Moissette et al. 2010; Frigui et al. 2016). The transition between the Tortonian interval and Messinian shows drastic lithology variations that correspond to intra-Tortonian and Early Messinian unconformities (Fig. 2). In the eastern area, the Segui Formation is characterised by interbedded clay and sand. Further north, the continental siliciclastics deposits of the Oued el Bir Formation are sandier with an average thickness of 100–200 m. These deposits may be related to the Messinian Salinity Crisis (MSC), occurring in 5.97 Ma in the Mediterranean (Grossi et al. 2011; Krijgsman et al. 2018; Mascle & Mascle 2019; Sciuto et al. 2020). The facies distribution of the Pliocene series was driven by a generalised transgression known as the Zanclean reflooding event, which occurred in 5.3 Ma. Additionally, 20 m thick bioclastic calcareous deposits are recognised along the Monastir cliffs. Benthic and planktonic foraminifera (*Globorotalia puncticulata*) allow a correlation with MPL4 Mediterranean planktonic foraminiferal zone interval (Arnould 1948; Colleuil 1976; Ben Salem 1992). Further to the north, yellow sand outcrops assigned to the Porto-Farina Formation are shown in the Nabeul-Hammamet hills with a thickness of 100 m. On land, the Mio–Pliocene outcrops are capped by a Villafranchian crust. The northeastern coasts are dotted with numerous Pleistocene high sea levels attributed to the last interglacial period. IRSL and OSL ages involve the occurrence of three distinct interglacial sea levels (MIS 9, MIS 7, and MIS 5) and are are calculated at 333±45 ka, 216±25 ka and 121±10 ka respectively (Elmejdoub & Jedoui 2009; Mauz et al. 2009; Mejri et al. 2012). The last high stand (MIS 5e) corresponds to the Tyrrhenian deposits represented by oolithic calcarenite and overlain by oolithic aeolian deposits (Mahmoudi 1988).

Fault population analysis

Methodology

The reconstruction of a palaeostress field requires a detailed tectonic analysis and kinematics of fault measurements (direction, dip, and pitch). According to Wallace & Bott's hypothesis, slickensides need to be parallel to the direction of the maximum resolved shear stress on the fault surface (Wallace 1951; Bott 1959). Numerical treatment according to the INVD method of Angelier (1991) is a handy tool to minimize the angle striae-shear and allows for the calculation of the shear stress direction on the fault. Integrating data from multiple faults was necessary for the calculation of paleostress tensor. Thus, 97 measurements of striated fault planes and joints were carried out in seven selected sites of the Late Miocene exposures in the Cap Bon Peninsula, Saouaf, Monastir, Jemmal, Zeramdine, and Ksour Essaf (Fig. 1). Table 1 shows the paleostress data calculated using the INVD. The orientations of

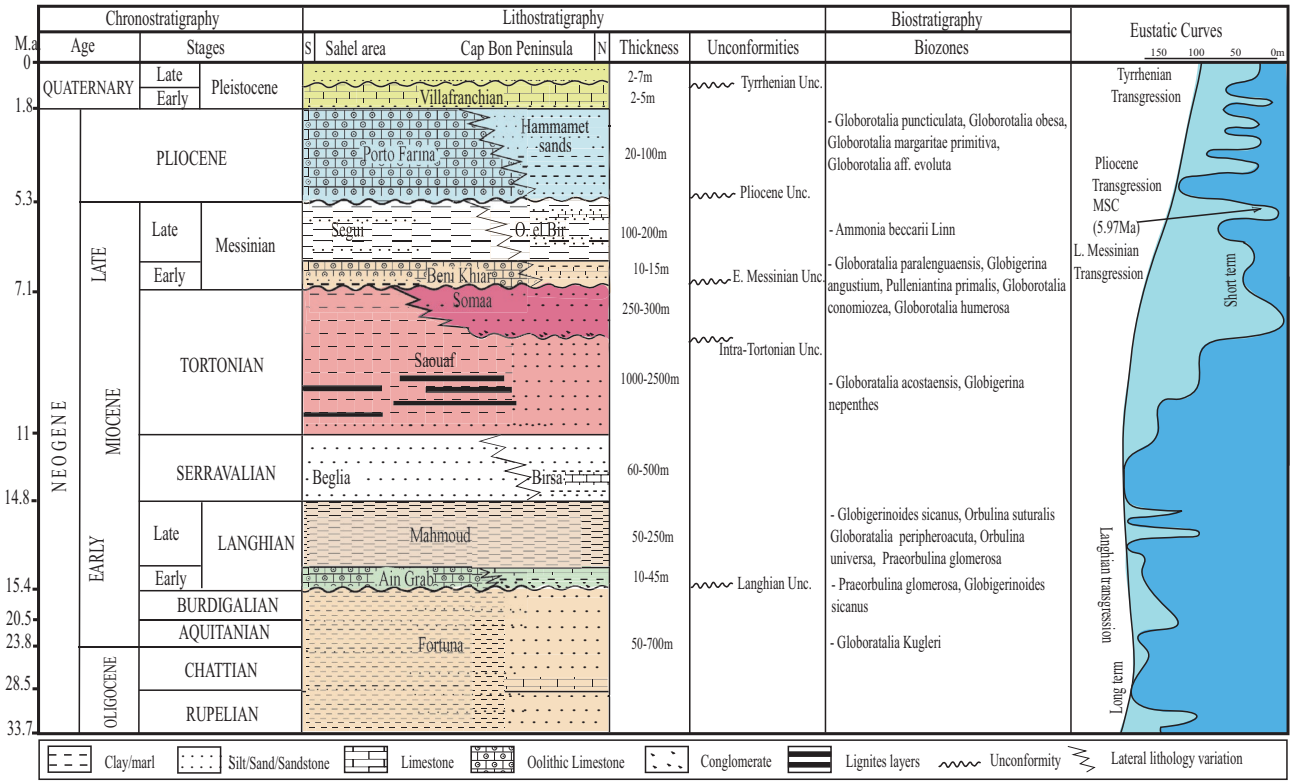

Fig. 2. Neogene–Quaternary stratigraphic chart of Sahel-Cap Bon area (not to scale) according to Berggren et al. (1995) and Frigui et al. (2016). Eustatic and relative sea-level changes after Haq et al. (1988). This paper refers to the time scale of Berggren et al. (1995). Planktonic forams are from Hooyberghs (1987, 1995), Besème & Blondel (1989), Hooyberghs & Ben Salem (1999), and Moissette et al. (2010).

faults, fractures, and paleostress determinations are drawn by stereoplots with lower hemisphere. Special attention was devoted to the temporal relationship among fault populations in order to distinguish different tectonic events. As another contributing factor to Late Miocene–Quaternary tectonic inversion, a comparison between Tortonian and Quaternary isopach maps was made to reconstruct the tectonic evolution of the eastern Tunisia during Late Neogene–Quaternary times. A strong relationship seems to exist among the oil and gas accumulations within the gulf of Hammamet and Late Miocene reactivated tectonics structures. The Tortonian (Birsa/Saouaf) trap configuration is constrained by well data correlation in northeastern Tunisia.

Extensional deformations

The outcrops of sandstones and clays of the Late Miocene, which occupy the western limbs of the Abderrahmane anticline in the Takelsa and Saouaf basins, record several centimetre scale syn-sedimentary normal faults. In many places, they are sealed by silts and sands of Messinian deposits (Fig. 3A, B). The conjugate faults found in the Saouaf basin exhibit orientations ranging from NW–SE to N–S, leading to tilted blocks and graben structures. The examination of sandy layers at the top of the Saouaf Formation yield to identify conjugate sets of cataclastic deformation bands. These fractures pass for a few meters presenting dominant NW–SE and NE–SW trends. The fracture pattern is compatible with the deduced stress field from fault measurements (Fig. 3C, D). To the south, in the Zeramdine–Jemmal quarries and along the Skanes–Monastir cliffs, Tyrrhenian deposits truncate the entire Tortonian succession. These later deposits are tilted to the east owing to the movement of NW–SE-trending faults (Fig. 3E). These fault planes show stepped slickenlines that pitch values varied between 70–80°, thereby indicating pure dip slip motion. These faults propagated eastwards forming several synthetic fault sets. Numerous horst and graben blocks buried by lignited layers of the Tortonian deposits are interweaved along syn-sedimentary normal faulting strikes (Fig. 3F, G, H).

The process of the fault analysis with the Angelier method allows for the determination of an extensional deformation with a maximum stress σ_1 nearly vertical and a minimum stress σ_3 trending N040.

Compressional deformations

In the investigated area of Monastir, E–W-trending thrust faults exhibiting low southward dips (40–50°) were measured. The slickensides on N090–100-trending faults planes lead to a compressional event with a maximum stress σ_1 oriented N–S (Fig. 4A). Further to the south, in addition to these reverse faults, a NE–SW anticline structure also exists that evolved through ductile conditions. The Tyrrhenian overlying sediments of Late Pleistocene age were not faulted. Unfortunately, the exact age of this deformation is poorly-constrained, perhaps related to Late Miocene to Early Quaternary movements (Fig. 4B). The Tortonian quarries of the Zeramdine and Jemmal offered the best opportunity to conduct a tectonic study. Several thrust faults were recognized in NE–SW direction with a decimetric to metric displacement (Fig. 4C, D). These faults juxtapose clay layers against sand beds and are overlain by the Segui Formation, where they are not cut by faulting. A compressional event with a maximum stress σ_1 trending N130–135 was deduced following the Tortonian deposition where fault activities ceased during Messinian times. Furthermore, the predominant direction of faulting shifts from NW–SE to E–W trending orientations in the vicinity of the Ksour Essaf–Mahdia area. Our field investigations reveal that this fault zone consists of multiple fault stands (Fig. 4E, F). These fault patterns are analogous to flower-shaped structures under a transpressional event with σ_1 oriented NW–SE and NE–SW trending σ_3.

Stress events chronology

The lower part of the Tortonian sequences outcrops in the Jemmal and Zeramdine quarries were affected by syn-sedimentary NW–SE trending normal faults that were sealed by

Table 1: Results of stress tensor determinations. The columns contain from left to right: NF – number of fault slip data; Trend or direction (D) and Plunge (P) of the principal stress axes (in degree); Φ – ratio $(\sigma_2–\sigma_3)/(\sigma_1–\sigma_3)$; α – average angle between computed shear stress and actual fault slip data (in degree); Rup – Internal quality coefficient (in percent); EXT – Extensional tectonic regime; COM – Compressional tectonic regime; SS – Strike Slip tectonic regime.

St.°		Location	NF	σ1		σ2		σ3		Φ	α	Rup	Tectonic regime
				D	P	D	P	D	P				
S1		Takelsa	15	65	70	145	16	**52**	11	0.439	11	16	**EXT.**
S2		Cap Bon Peninsula	12	04	79	140	08	**51**	07	0.279	6	17	**EXT.**
S3		Saouaf	10	119	73	137	04	**40**	17	0.088	9	12	**EXT.**
S4	a	Monastir	6	10	83	120	03	**30**	06	0.226	10	21	**EXT.**
	b		6	**177**	09	87	05	167	81	0.687	8	14	**COM.**
S5	a	Zeramdine	18	132	73	144	17	**53**	03	0.426	10	15	**EXT.**
	b		15	**115**	08	52	02	14	81	0.501	12	19	**COM.**
S6		Jemmal	7	**145**	04	33	05	74	84	0.459	8	9	**COM.**
S7		Ksour Essaf	8	**135**	10	133	25	**46**	22	0.723	5	10	SS.

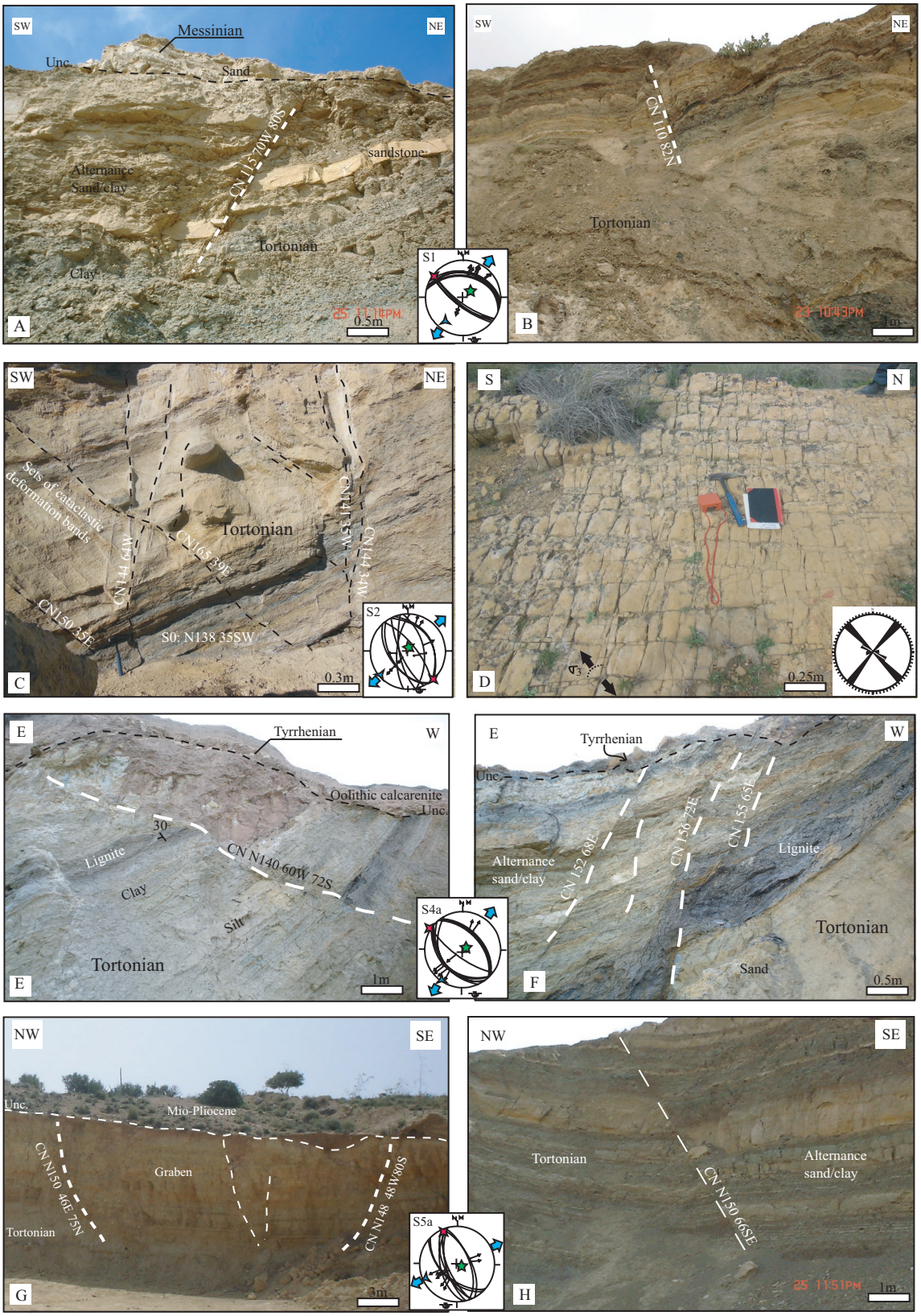

Fig. 3. Photographs showing the syn-Miocene extensional deformations: **A, B** — N110–150 trending normal faults related to NE–SW extension (Takelsa site); **C** — Conjugate NW-trending normal faults created graben structures and tilted blocks (Saouaf site); **D** — NE and NW-trending sets of joints (Saouaf site); **E, F** — NW-trending normal fault sealed by Tyrrhenian deposits related to NE–SW extension (Monastir site); **G** — Graben structure created by conjugate NW–SE-trending normal faults; **H** — Metric offset induced by NW-striking faulting. They exhibit slip surface indicating pure dip slip normal motion (Zeramdine site).

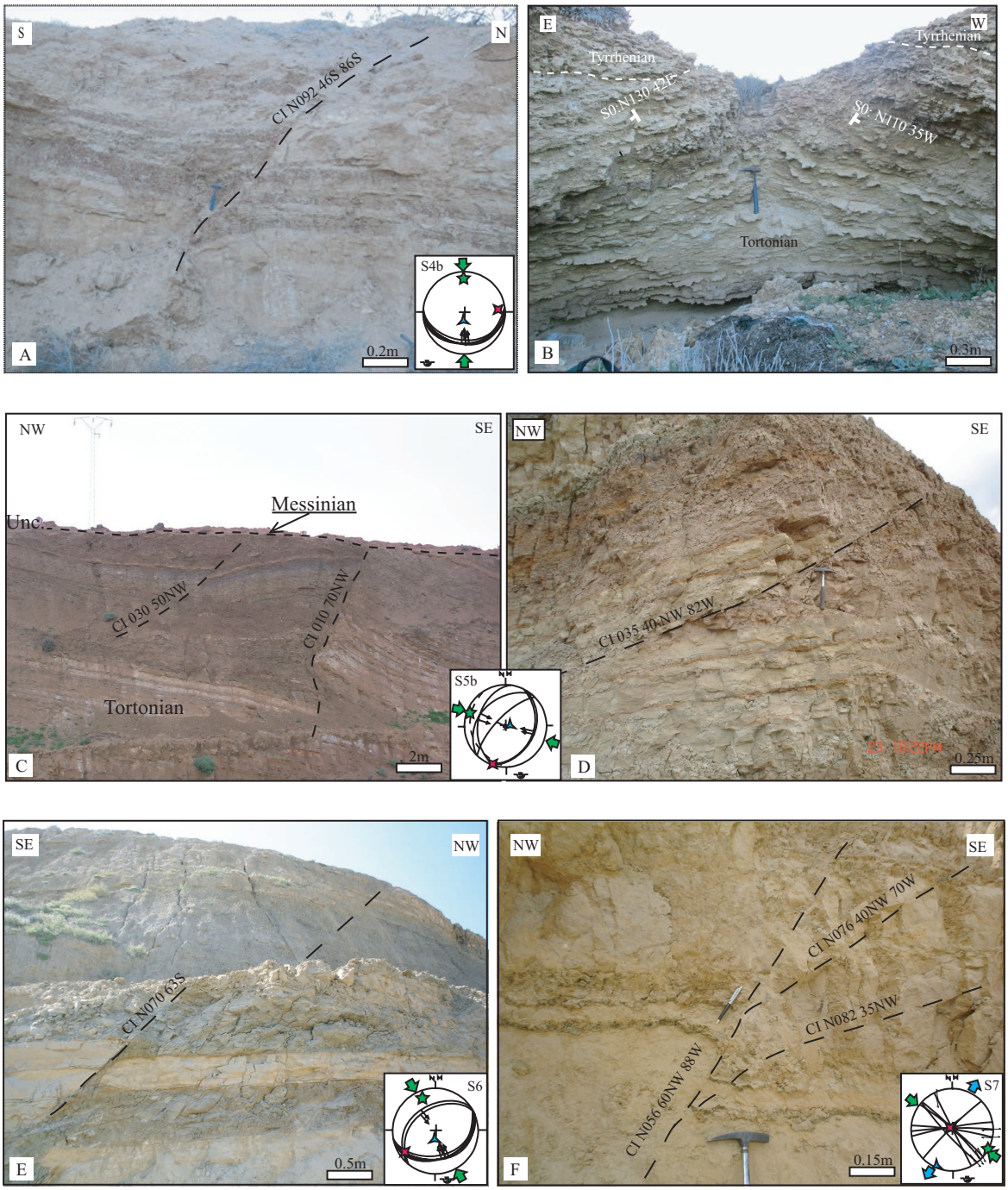

Fig. 4. Photographs showing the post-Tortonian compressional deformations: **A** — NNW-directed post-Tortonian compression indicated by NE–SW-striking low-angle thrust faults (Monastir site); **B** — NE–SW folded structure sealed by Tyrrhenian deposits (Monastir site); **C, D** — Metric displacement thrust faulting related to ESE–WNW trending compression (Zeramdine site); **E** — Northeast striking faults with thrust kinematic indicators (Jemmal site); **F** — East striking faults system form flower structure (Ksour Essaf site).

the Messinian continental siliciclastic deposits attributed to the Segui Formation. The thickness of the Tortonian deposits implies that the Saouaf Formation was deposited on syncline areas with a great tectonic subsidence rate, which occurred in the Sahel area and the Cap Bon Peninsula (Fig. 5A, B). Several lignite beds recognised in the Zermadine and Jemmal quarries were developed under syn-tectonic structuration and combined to the eustatic sea level variations and climatic changes. The associated vertical fractures affected the sand and clay alternates of Tortonian sequences, as well as intersect with the NW-trending fault patterns with a gentle angle (Fig. 5C). The Tortonian thickness increases towards the south-west where basin-controlling faults suggested syn-sedimentary deformation. These synthetic faults and fractures

were generated by an extensional event with the NE–SW trending σ_3. Further westward of the investigated area, the upper beds of the Tortonian deposits were folded and truncated by the horizontal Messinian layers (Fig. 5D). These outcrops show an asymmetrical fold with an axis orientation N40°E, demonstrating that the main folding episode occurred during the post-Tortonian times and priori the Messinian unconformity interface. Furthermore, to the north in the Monastir area, a fault outcrop provides several vertically-stepping echelon normal faults belonging to the WNW–ESE striking. The thickness increase in hanging wall of fault zone indicates syn-sedimentary displacement associated with clear evidence of smeared shale. In the higher part of the fault zone, an ENE–WSW striking low-angle thrust fault reactivated the former extensional faults (Fig. 5E). Southward, in the vicinity of Zeramdine, several NW–SE normal fault surfaces contain different sets of calcite, gypsum fibers, and lunate tectoglyphs showing subvertical, as well as locally sub-horizontal striae. They indicate that left-lateral striation overprinted upon the ancient normal striae. The above observations evidence two stages of faulting, which started with syn-sedimentary normal movement that was later reactivated with reverse component in post-Tortonian times. These fault patterns were sealed by the early Messinian unconformity in space, corresponding to ~7.1 Ma in time.

2D seismic data

Input data description

A total of 212 2D-seismic lines, covering an area of 6900 km^2 located between 35°–35°40N and 10°10–11°10E, were investigated on the Sahel area (Fig. 6). The data set comprises also 30 wells collected from the Entreprise Tunisienne d'Activités Pétrolières (ETAP). The wells are located along the studied seismic lines, allowing for a remarkable calibration and drilled through the formations ranging from Quaternary to Triassic. Using CHARIZMA station software, the interpretation of seismic and detailed well data was conducted. Two selected reflectors of Late Miocene and Quaternary were marked on the seismic lines. The depth of each seismic reflector calculated on the basis of two-way travel time (TWTT) of the seismic line was correlated with well tops to generate time structure maps of the study area. Time of the isopach maps was correlated with well tops data and thicknesses of rocks, in terms of metres (m), were calculated. Application of the flattening technique allowed for two-dimensionally structural evolution and sedimentary filling of the Sahel area.

Deep Miocene structure

The seismic profile L1 in the Grombalia graben at the southern part of Cap Bon Peninsula reveals an important regional unconformity intra-Tortonian in age that marks the boundary between the Somaa (Late Tortonian) and Saouaf (Early Tortonian) sequences (Fig. 7). This intra-Tortonian unconformity interface truncates underlying strata of Tortonian age and leads to the Somaa conglomerate deposition where several toplaps are shown. Its formation is related to a large-scale structural inversion in which early Tortonian deposits were considerably affected by the erosion. This tectonic unconformity seals faulted as well as partially-eroded and thin Neogene deposits. The earlier faulting produced domino-type features, which exhibited listric-shaped patterns and controlled the deposition of the Saouaf Formation. At the south-western boundary of the Grombalia graben, the Grombalia fault exhibits a normal S-shape pattern. These Late Miocene sedimentation-controlling faults indicate flower-shaped structures. Variation thicknesses across the faults suggest a predominantly extensional movement. Furth to the south, the importance of the tectonic inversion in the northern part of Tunisian Sahel that controlled the Miocene and Quaternary structuration was disclosed by the seismic profile (L2; Fig. 8). At least two stages of faulting were identified in the last 11 Ma and started with high-angle conjugated normal faulting that formed horst and grabens. The notable throw was documented along the Jemmal–Zeramdine faults system where the faulting blocks controlled Miocene depositional sequences. The second faulting stage corresponds to an important compressional event that began in post-Tortonian times and is accentuated by the youngest episode of deformation which occurred during the late Pliocene–early Quaternary (post-Villafranchian compression). The majority of pre-existing faults, such as the el Hadjaja fault system, which affected Tortonian and Langhian sequences, were reactivated with a reverse slip component forming a positive flower structure. The subsequent contractional deformation uplifted the Msaken area located between the el Hadjaja fault and Jemmal–Zeramdine fault zones. It is important to note that the crest of the Quaternary inverted structures nearly coincides with the former Tortonian basins as a consequence of the pre-existing faulting reactivation.

Interpretation of isopach maps

Late Miocene isopach map

The isopach map of the Late Miocene sequences on the basis of time is provided in Fig. 9. The thickness range of the Late Miocene reflector in terms of TWTT-contour map is 1600 ms to 2380 ms. Several northwest–southeast-trending elongated depocenters, tens of kilometers long, can be recognised (Fig. 9A). The subsidence rate recorded in the Monastir and Zermadine syn-depositional areas was induced by a huge sediments thickness reaching 1000 m. The progressive southward deepening of Tortonian facies is where three well-defined isolated Tortonian depocenters can be easily recognised in the south of Chorbane, Jem, and Hencha–Bouthadi areas. The superposition between Late Miocene isopach contours and fault trends deduced from our seismic reflection data of eastern Tunisia (Sahel area) show that the morphology of

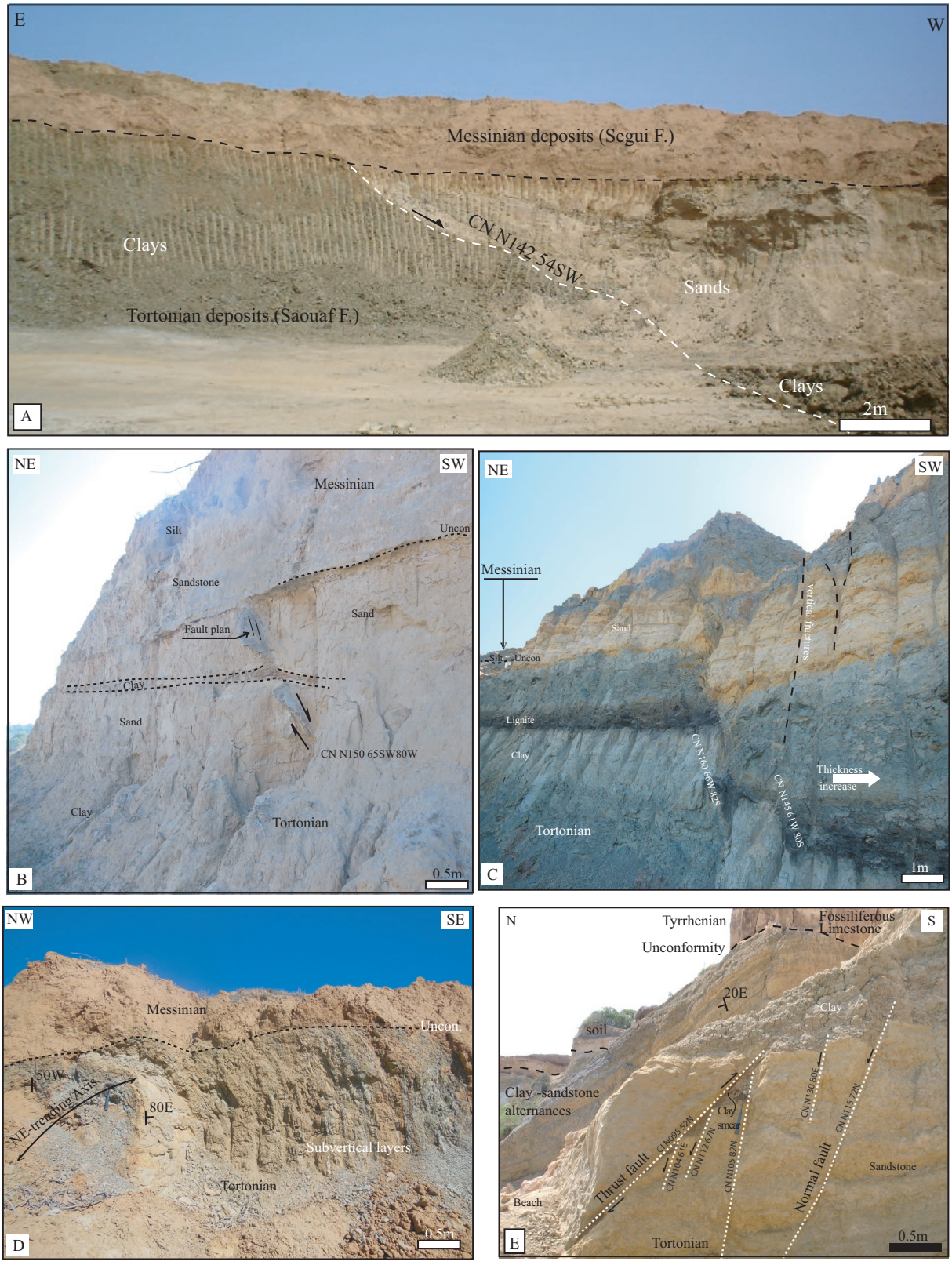

Fig. 5. Panel photos underline the chronology relationship among deduced tectonic events: **A** — Syn-sedimentary normal fault affected the Tortonian formation and sealed by the Messinian deposits (Jemmal site); **B, C** — NW–SE-trending normal faults and fractures shaped a half-graben structure where the thickness of Tortonian increases to the west (Zeramdine site); **D** — Asymmetrical Tortonian fold, N45°E-trending axis, sealed by the Messinian deposits (Zeramdine site); **E** — Field tectonic inversion of northwest striking normal displacements by low-angle thrust fault (Monastir site). These distinct events are sealed by the Tyrrhenian deposits.

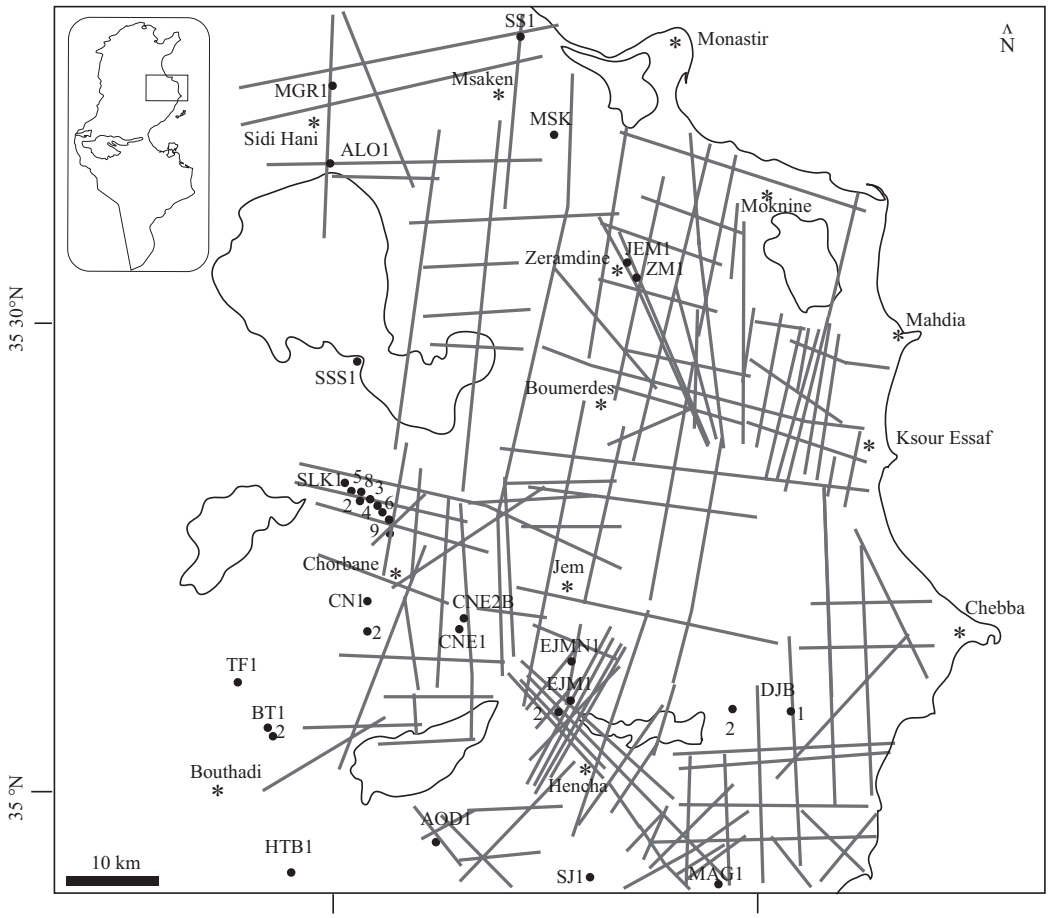

Fig. 6. Location map of 2D seismic profiles and wells used in the study.

these sedimentary basins are controlled by NW–SE tectonic trends. The Skanes–Monastir trough deepens towards the south-west, reaching a maximum Tortonian thickness of about 900 m, which is controlled by the south-dipping normal fault of Monastir. Its strike changes progressively from a NNW–SSE to NW–SE direction, linking southward to the Zeramdine fault zone. This fault zone forms 3 to 5 km wide and consists of multiple fault segments. These conjugate normal faults separated the Zeramdine graben from the nearby Moknine horst where no Tortonian strata deposition is shown (Fig. 9B). The interpreted seismic reflection profiles show the Mahdia zone to be from a major horst feature that resulted in the erosion of Tortonian deposits. Towards the south, these deposits are limited to the nearby Ksour Essaf fault-controlled basin.

Plio–Quaternary isopach map

The Plio–Quaternary sedimentation is influenced by the post-Messinian structuration and illustrated on several regional seismic lines. The Plio–Quaternary reflector has a maximum thickness of about 2600 ms TWTT in the areas of Jem and Monastir. Significant depocenters migration can be observed in the Mahdia and Bekalta areas. Moreover, it is important to note that the inverted structures are concentrated near the southern area of eastern Tunisia, especially in the areas of Zeramdine and south of Chorbane, which experienced significant neotectonic uplift and local folding with a wavelength of about 30 km. These areas witnessed the Quaternary tectonic inversion of Late Miocene syn-rift structures (Fig. 10A). Southwards, some faults displayed subparallel alignments trends, such as the el Hadjaja, Mahdia, and Chorbane E–W-striking faults. The coexistence of NE–SW-striking thrust faults and E–W strike slip-fault trends are analogous to fault patterns in the dextral oblique model and may be the main mechanism responsible for the Tortonian basin inversion in eastern Tunisia. It should also be noted that the N–S-trending Jem fault is interpreted as Riedel's shears fractures under transpressional movements (Fig. 10B).

Discussion

Tectonic-related lithofacies and thickness variation of Tortonian sequences

The Late Miocene facies evolution of the Sahel–Cap Bon Peninsula is governed by its paleogeographic setting, sea-level

oxcillations, paleoclimatic conditions, and structural evolution (Salaj & Stranik 1970; Hooyberghs & Ben Salem 1999; Ben Moktar & Mannaï-Tayech 2011). They are developed with various thicknesses and facies. According to the information from the wells and outcrops in the studied area, abundant sandy layers intercalated with thick mudstone, where the study area hosts large basins receiving terrigenous sediments from the Atlassic belts by river and delta systems (Mannaï-Tayech et al. 1992). Here, the Tortonian sequential outcrops of the Zeramdine become more lignitiferous, further showing a strong correlation between lithofacies and tectonic subsidence. The thickening Tortonian sequences (1000–2000 m) were

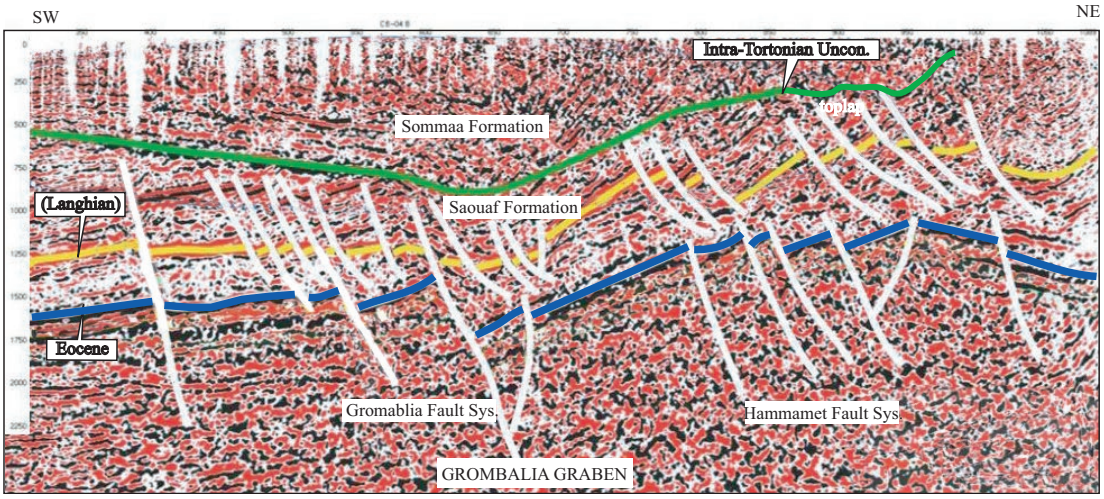

Fig. 7. Interpreted seismic section across the Grombalia graben L1 (see Fig 1 for location) reveals that an important tectonic intra-Tortonian unconformity sealing the faulted and partially eroded Tortonian sequences. Synsedimentary NW trending faults exhibit listric-shaped pattern on the Grombalia graben (modified from Abidi et al. 2014).

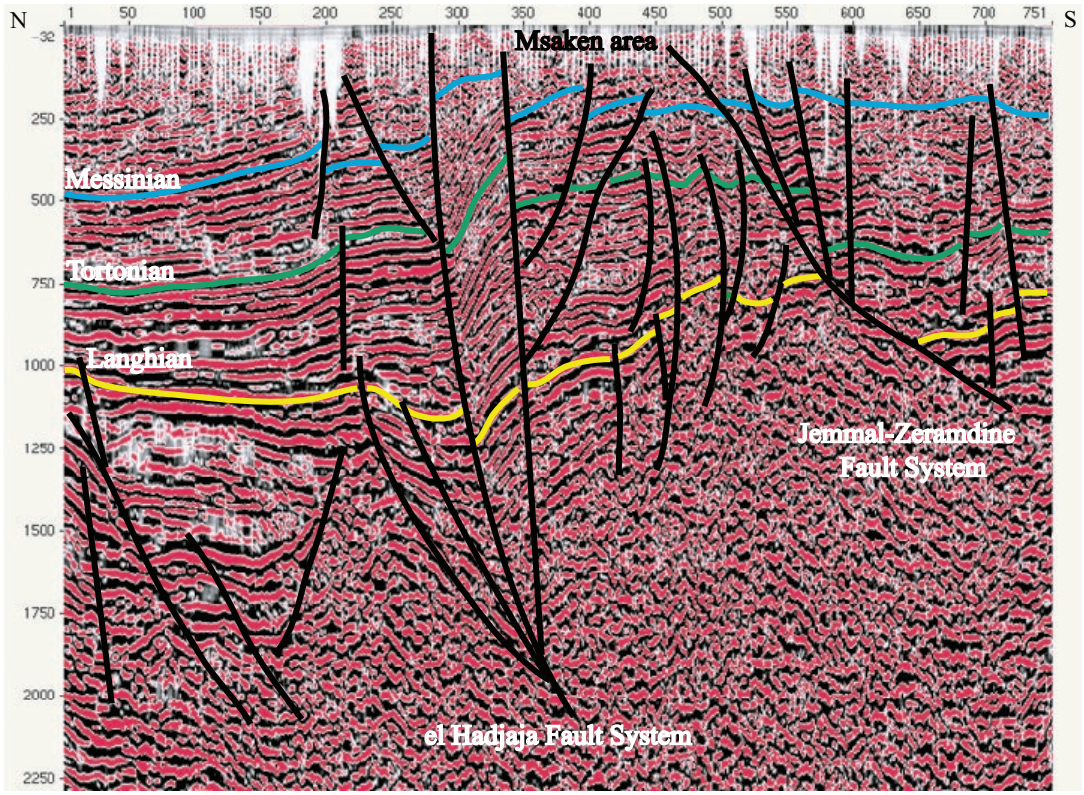

Fig. 8. Interpreted seismic profile L2 (see Fig. 1 for location) provides clues on the evolution of Late Miocene to Quaternary faulting in Tunisian Sahel. Note the positive flower structure of the el Hadjaja and Jemmal–Zeramdine fault systems that uplifted the Msaken area.

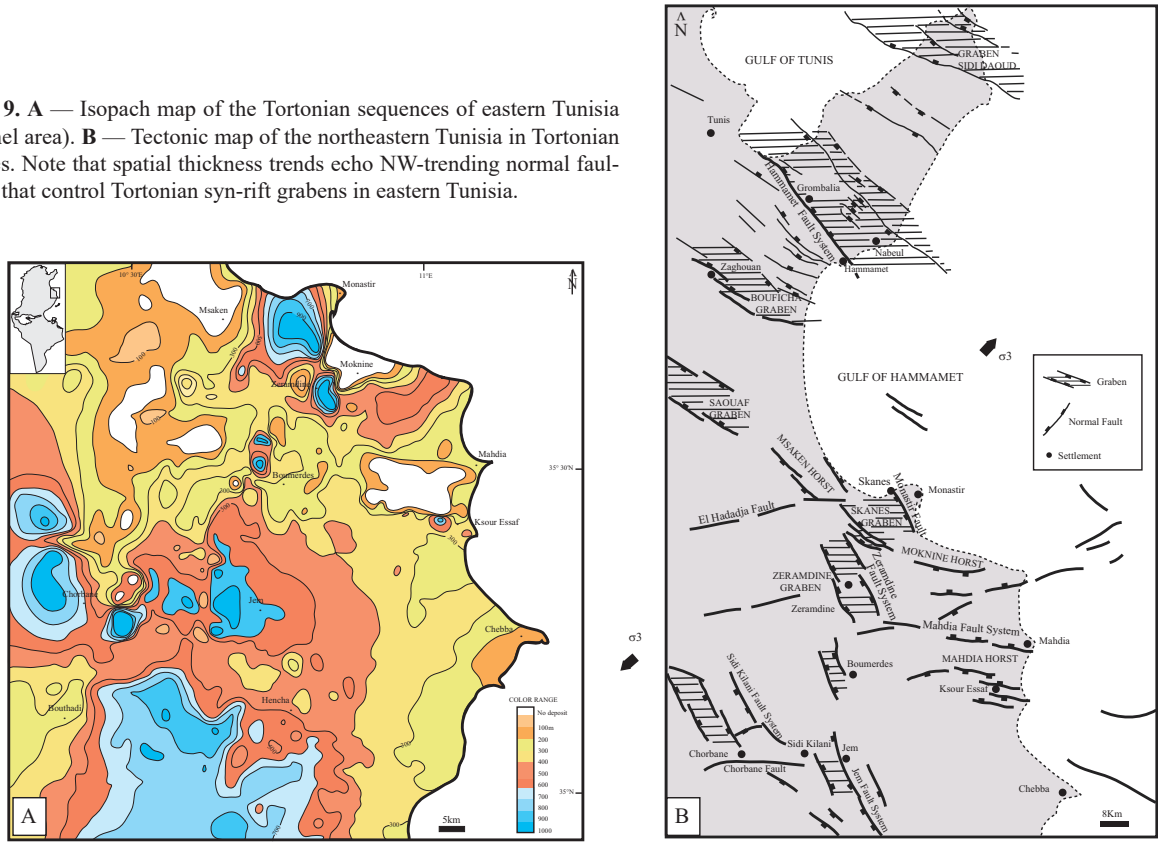

Fig. 9. A — Isopach map of the Tortonian sequences of eastern Tunisia (Sahel area). **B** — Tectonic map of the northeastern Tunisia in Tortonian times. Note that spatial thickness trends echo NW-trending normal faulting that control Tortonian syn-rift grabens in eastern Tunisia.

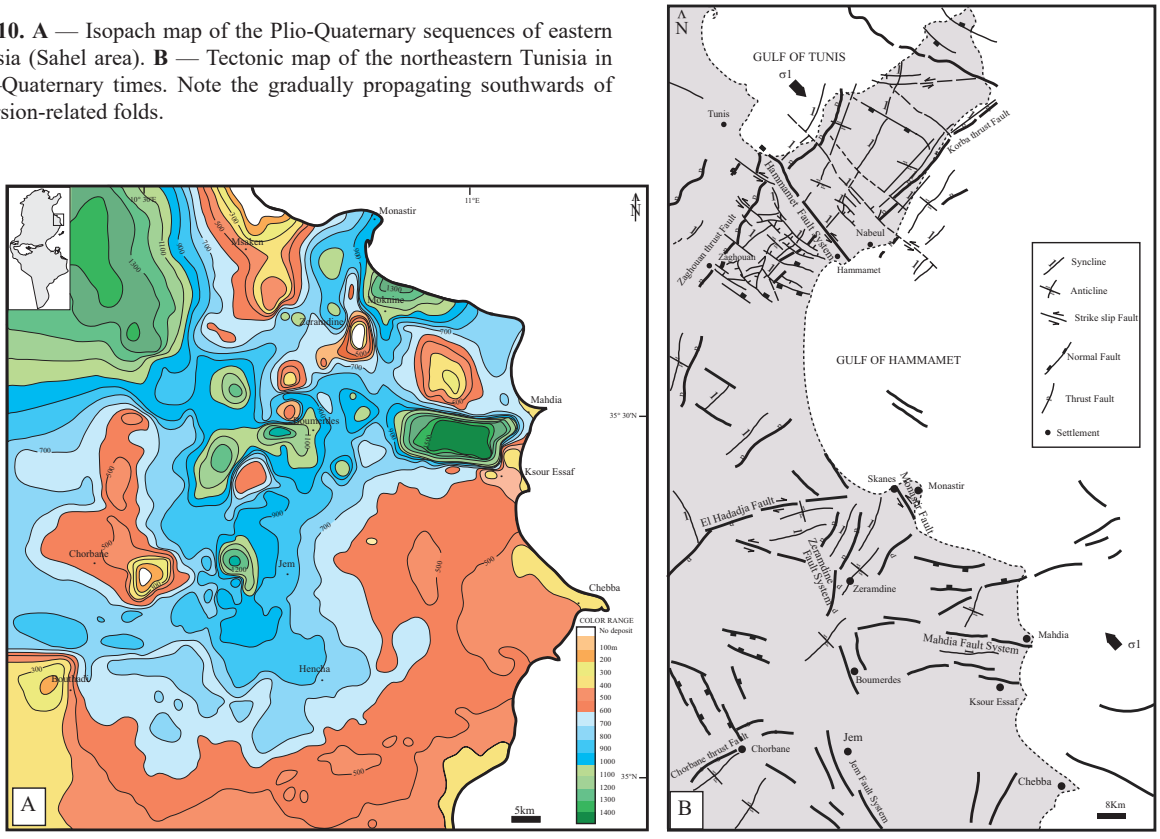

Fig. 10. A — Isopach map of the Plio-Quaternary sequences of eastern Tunisia (Sahel area). **B** — Tectonic map of the northeastern Tunisia in Plio–Quaternary times. Note the gradually propagating southwards of inversion-related folds.

deposited within the areas of subsidence in Monastir and Zeramdine. The geometry of these deep basins is influenced by the activity of the Skanes–Monastir fault and Zeramdine fault system, respectively. Further northwestward of the investigated area, the Tortonian thickness decreases gradually where only a few meters are present in the SS1 well. This area corresponds to a Horst block of Msaken shaped by the el Hadjaj fault system (Fig. 11). Southward, the Tortonian depocenter within the Boumerdes area is separated by Mahdia and Sidi Kilani, acting as E–W trending elongated paleohighs through Tortonian times. These highs and basins are a hectometric to kilometric extension, corresponding to horsts and grabens limited by NW to N trending faults of Boumerdes and Sidi Kilani. The application of the flattening method on the Sidi Kilani–Boumerdes–western part of Mahdia area suggests that the first key component of the Late Miocene tectonic history is the syngenetic tectonic movements along normal faults and underlines by the readjustment along pre-existing N-trending faults. Some of these faults belong of the pre-existing late Cretaceous faults, such as the Boumerdes fault zone. They controlled the deposition and thickness of the Tortonian deposits within the Sidi Kilani–Boumerdes area (Fig. 12). A subsurface study conducted by Bedir et al. (1996) suggested that Serravalian to Tortonian deposition in Tunisian Sahel occurred in the transtensional pull-apart graben located at the intersection between the E–W and NE–SW striking structures. These extensional structures were characterised by Miocene calc-alkaline volcanism contoured in wells of the Sahel area (Rouvier 1977; Laaridhi-Ouazza & Bedir 2005; Halloul & Gourgaud 2012; Decrée et al. 2014).

Late Miocene–Quaternary inversion-related structures

The Sahel–Cap Bon Peninsula reveals a significant reduction in the magnitude of the tectonic subsidence, starting in Messinian times and continuing through the Late Pliocene and Quaternary. The relationship between the lower Tortonian sediments and the uppermost Tortonian sequences constitutes a strong regional unconformity by the fact that the Somaa deposits (Late Tortonian) are clearly discordant over the early Tortonian sediments. Without any doubt, after the deposition of the early Tortonian sediments, a strong pulsation took place, as is shown in several seismic sections and by field investigation. The reverse kinematics and strike-slip motions of the ENE–WSW to E – W trending faults crosscutting the Tortonian deposits induced normal fault reactivation and uplift. At that

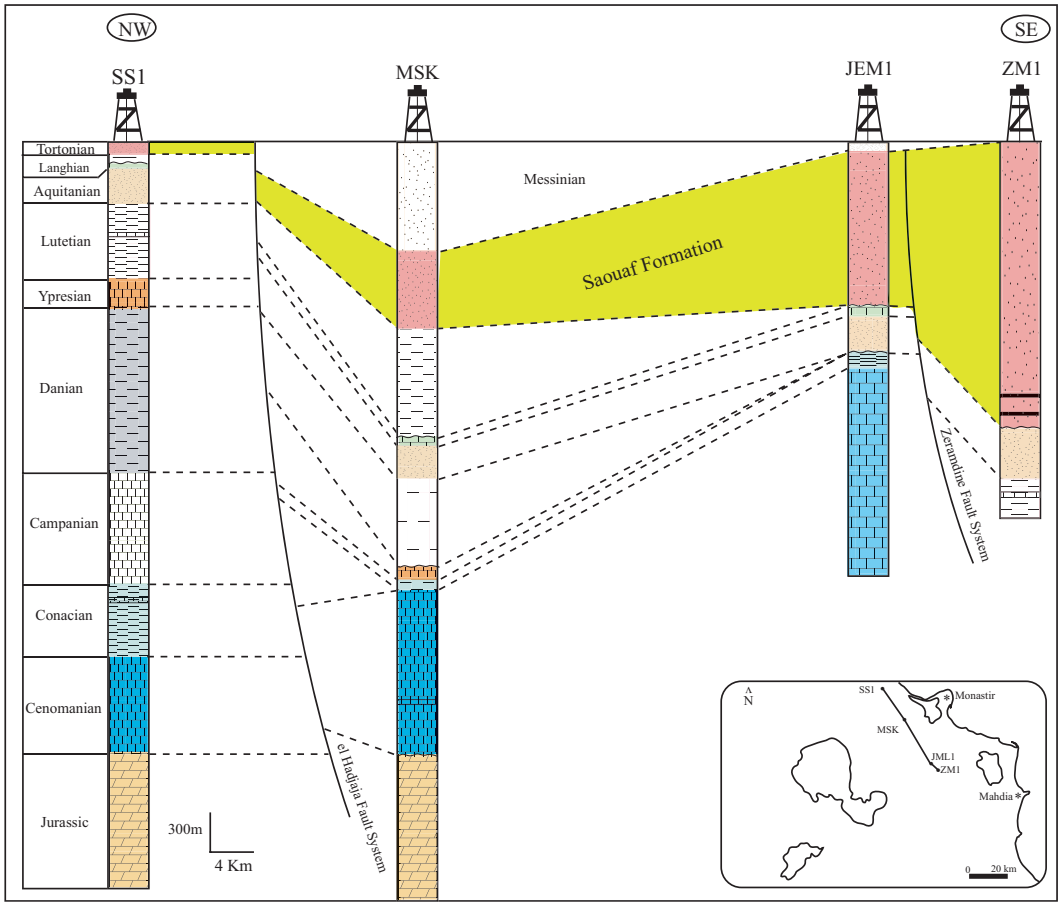

Fig. 11. NW-trending well correlation shows thick succession of the Saouaf Formation within the Zeramdine and Jemmal synclines. The Tortonian thickness variations were controlled by the Zeramdine and el Hadjaja faut systems.

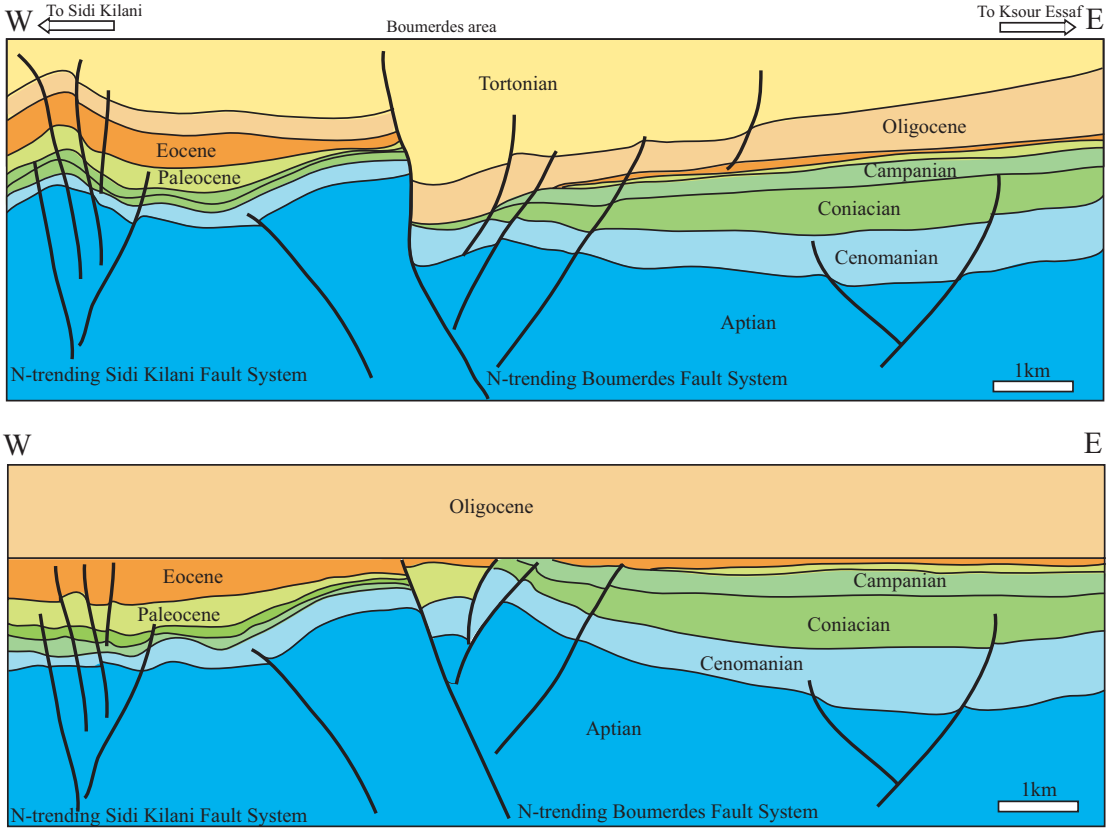

Fig. 12. Two dimensionally structural evolution of the Boumerdes area after flattening the Oligocene horizon. Note the deep Tortonian basin of Boumerdes controlled by normal faulting. Westwards, the reduced Tortonian sedimentation was influenced by Sidi Kilani fault system.

time, the Rif's belt emerged and ceased communication between the Atlantic and Mediterranean. The N-directed plate convergence was responsible for the Messinian Salinity Crisis (MSC) occurring in the occidental Mediterranean (Letouzey & Trimoliere 1980; Weijermars et al. 1985; Morel 1989; Vissers et al. 1995; Augier et al. 2013). The contractional processes are coeval with extensional deformations operated in mainly Mediterranean areas like the Tyrrhenian Sea. The Pliocene extensional structures are suborthogonal towards the Plio–Quaternary shortening direction (Sartori et al. 2001; Booth-Rea et al. 2018). The stress inversion of focal mechanisms allowed for the definition of a NW–SE to NNE–SSW transtensional regime in the Cap Bon Peninsula (Grombalia area), as well as a transpressional tectonic regime with a NW–SE-oriented sigma1 axis in the Hammamet offshore and the Monastir area (Chihi et al. 2000; Ghribi et al. 2018; Soumaya et al. 2018). These data correlated with the Quaternary in-situ stress measurements (Ghribi & Bouaziz 2010) and with the average S_{Hmax} orientation on the Word Stress Map.

Upper Miocene hydrocarbon potential

N–S offshore wells correlation of the Miocene sequences show that the Birsa/Beglia and the Lower Saouaf sandstones exhibit notable variations in thickness and lateral kilometric extension. The Tazerka concession where the W1 well is drilling shows thick Birsa sequences related to subsiding graben bordered by the NW-trending Tazerka fault. Further to the south, these sequences started to decrease on the Birsa concession, as well as to the S-edge of the Tazerka concession. The reduced Birsa/Tortonian deposits are controlled by the uplift of the Birsa area where a push up structure and NE–SW drag fold related to the tectonic inversion are being drilled by the W3 well (Fig. 13A). These sequences are more developed to the South of the Oudna concession (W4) than the area where the W5 is drilling. The present-day trap configuration of the Oudna concession had already been created during the Late Miocene extensional tectonic and was strongly affected by the NW–SE trending "Atlassic" tectonic inversion. The later event was responsible for the reactivation of E-trending syn-sedimentary normal faulting to thrust trends as the Oudna thrust fault (Fig. 13B). The deposition of the Birsa sequences was influenced by sea-level oscillations. The depositional model suggests a fluvio-deltaic environment where the spatial distribution of Birsa sandy channels was dictated by the geometry of Miocene horst and graben systems. These later structures witnessed a Late Miocene tectonic subsidence by normal faulting (Bedir et al. 2016).

In terms of prospect, the Gulf of Hammamet was considered the highest prospective area where the majority of oil and gas

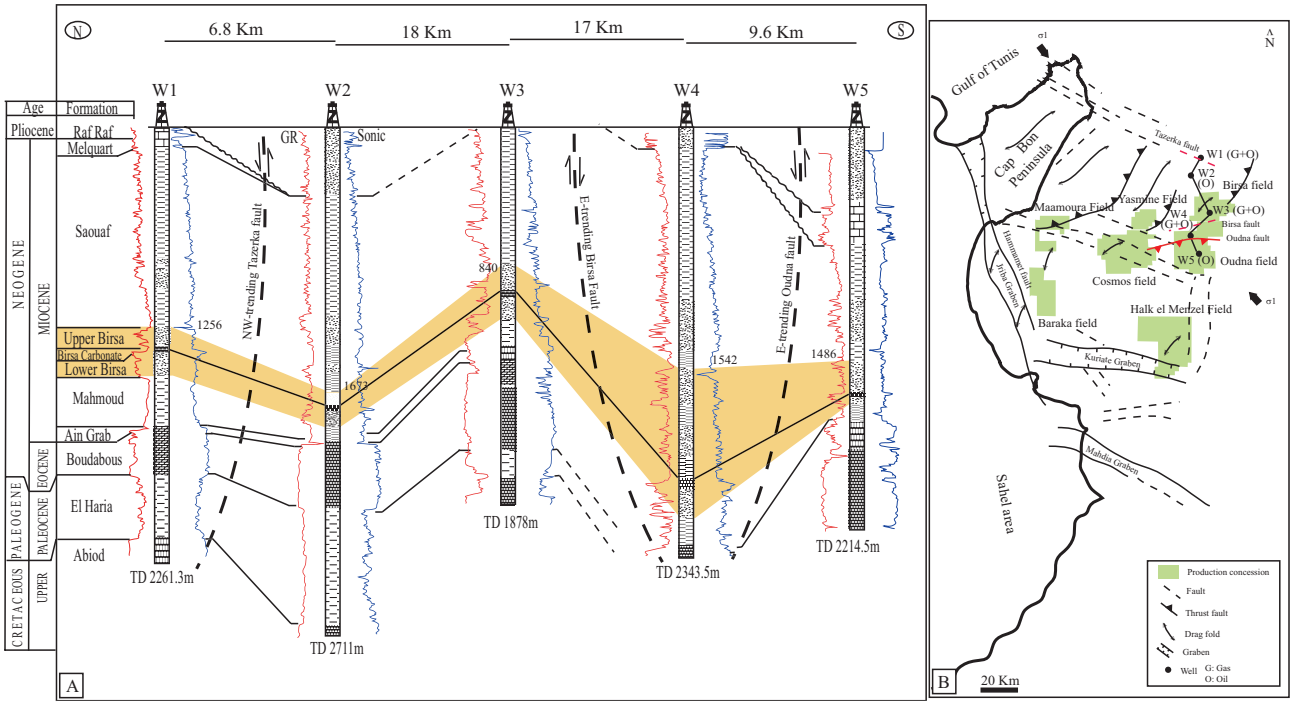

Fig. 13. A — Lithostratigraphic correlation between W1, W2 (Tazerka field), W3 (Birsa field), W4 and W5 wells (Oudna field); **B** — Offshore structural map of northeastern Tunisia. Note the N–S facies and thickness variations of Birsa sand reservoir over the Hammamet basin related to tectonic trends.

discoveries were hosted (Tazerka, Oudna, Birsa). The Birsa sands can be divided into two distinct units (Upper and Lower units) separated by the intra Birsa carbonate. Only the Upper unit of the Birsa sands are a major target with good porosity (10 to 33 %) and a permeability above 1 Darcy. The Lower Tortonian trap geometry accumulates oil and gas expulsed from the Cretaceous source rocks. The shaly intercalation of the Late Tortonian acted as a potential seal for hydrocarbon plays. The main episodes of petroleum generation and migration took place during Miocene to Pliocene times (Ouahchi et al. 2002).

Conclusions

The Upper Miocene outcrops, which are recognised as the Saouaf Formation, are well-developed in the Zeramdine, Monastir, Saouaf, and Takelsa basins. They documented syn-depot NE–SW trending extensional tensor. Titled blocks, horsts, and grabens created subsiding areas where thicker Late Miocene sequences were deposited. The intra-Tortonian extensional event was followed by a NW–SE directed post-Tortonian compressive stress-field taking place during the Neogene basin history (Atlasic orogeny). Their morphological expressions are NE–SW striking folds, and larger scale uplifts overprint the north-eastern topography. Overall, several thrust faultings are recognised in offshore and onshore areas, indicating that the Late Miocene tectonic inversion of syn-rift structures where gentle compressional or transpressional folds are highlighted by seismic sections and field investigations. They associated with an important regional unconformity intra-Tortonian in age that marks the boundary between the Somaa (Upper Tortonian) and Saouaf (Lower Tortonian) formations. The ongoing shortening of the Africa and Europe plates in Plio–Quaternary times is underlined by an accentuation of the previously-described Tortonian structures. The inverted structures known in Hammamet offshore provided the most attractive traps for significant oil and gas discoveries (Tazerka, Oudna, Birsa) where the Tortonian sandstones (Birsa/Beglia and Lower Saouaf) are the most important targets in north-eastern offshore Tunisia. They exhibit considerable variations in thickness controlled by Late Miocene to Quaternary tectonic trends.

Acknowledgments: We thank two anonymous reviewers, as well as Michal Šujan and Silvia Antolíková for their useful comments and suggestions, which increased the scientific value of the manuscript by many folds.

References

Abidi O., Inoubli M.H., Sebei K., Boussiga H., Amiri A. & Nasr I.H. 2014: Geodynamic framework and petroleum potential of the Cap Bon–Gulf of Hammamet province – Tunisia. *Search and Discovery Article*, 30368.

Angelier J. 1991: Inversion directe et recherche 4-D: Comparaison physique et mathématique de deux modes de détermination des tenseurs des paléocontraintes en tectonique cassante. *Les plans de défaut non cisaillants ou "non-faille"* 314, 381–386.

Arnould M. 1948: Les formations pliocènes marines de la péninsule du Cap Bon (Tunisie) Région d'Oum Douil. *Comptes rendus sommaires des séances de l'Académie Géologique de France*, Paris, 215–216.

Augier R., Jolivet L., Do Couto D. & Negro F. 2013: From ductile to brittle, late to post-orogenic evolution of the Betic Cordillera: Structural insights from the North-eastern Internal Zones. *Bulletin de la Société Géologique de France* 184, 405–425. https://doi.org/10.2113/gssgfbull.184.4-5.405

Azizi R. & Chihi L. 2016: Superposed folding in the Neogene series of the northeastern Tunisia: Precision of the upper Miocene compression and geodynamic significance. *International Journal of Earth Sciences* 106. https://doi.org/10.1007/s00531-016-1394-0

Azizi R. & Chihi L. 2021: Neogene basin of Northern Tunisia: new evidence of graben structures along E–W shear zone and geodynamic implications. *International Journal of Earth Sciences* 110. https://doi.org/10.1007/s00531-021-02077-x

Bedir M., Tlig S., Bobier C. & Aissaoui N. 1996: Sequence stratigraphy, basin dynamics and petroleum geology of the Miocene from eastern Tunisia. *Notes Service Géologique de Tunisie* 80, 63–81.

Bedir M., Arbi A., Khomsi S., Houatmia F. & Aissaoui M.N. 2016: Seismic tectono-stratigraphy of fluvio-deltaic to deep marine Miocene silicoclastic hydrocarbon reservoir systems in the Gulf of Hammamet, northeastern Tunisia. *Arabian Journal Geosciences* 9, 726. https://doi.org/10.1007/s12517-016-2745-7

Ben Ayed N., Viguier C. & Bobier C. 1983: Les éléments structuraux récents essentiels de la Tunisie nord-orientale. *Notes du Service Géologique de Tunisie* 47, 5–19.

Ben Ferjani A., Burollet P.F. & Mejri F. 1990: Petroleum Geology of Tunisia. *ETAP memoir* 1, Tunis, 1–194.

Ben Ismail-Lattrache K. 1981: Etude micropaléontologique et stratigraphique des séries paléogènes de l'anticlinal du Djebel Abderrahmane (Cap Bon, Tunisie nord-orientale). *Thèse 3ème cycle, Université. Tunis II. Faculté des Sciences*, 1–224.

Ben Moktar N. & Mannaï-Tayech B. 2011: Reconstitution de la végétation et du climat durant le Miocène dans le bassin de Saouaf (Tunisie centro-nord orientale). *Géodiversitas* 34, 445–456. https://doi.org/10.5252/g2012n2a11

Ben Moktar N. & Mannaï-Tayech B. 2012: Palynology and sedimentology of the Miocene series in the north-east of Tunisia: the climatic and eustatic signature. *Arabian Journal of Geosciences* 7, 385–396. https://doi.org/10.1007/s12517-012-0808-y

Ben Romdhane M., Brahim N., Ouali J. & Mercier E. 2006: Tectonique quaternaire et plis de rampe dans le golfe d'Hammamet (offshore tunisien). *Comptes Rendus Géoscience* 338, 341–348.

Ben Salem H. 1992: Contribution à la connaissance de la géologie du Cap Bon: stratigraphie, tectonique et sédimentologie. *Unpublished Ph.D. Thesis, University of Tunis*, 1–155.

Berggren W.A, Kent D.V., Swisher III C.C. & Aubry M.P. 1995: A revised Cenozoic geochronology and chronostratigraphy. In: Berggren W.A., Kent D.V., Aubry M.-P. & Hardenbol J. (Eds.): Geochronology, Time Scales and Global Stratigraphic Correlations. *Society of Economic Paleontologists and Mineralogists Special Publication* 54, 129–212.

Besème P. & Blondel T. 1989: Les séries à tendance transgressive marine du Miocène inférieur à moyen en Tunisie centrale: données sédimentologiques, biostratigraphiques, et paléoécologiques. *Revue Paléobiolologie* 8, 187–207.

Besème P. & Kamoun Y. 1988: Le Messinien marin de Ksour Essaf (Sahel, Tunisie orientale), une étude stratigraphique, sédimentologique et paléoécologique. *Revue des Sciences de la Terre* 8, 129–142.

Biely A., Rakús M., Robinson P. & Salaj J. 1972: Essai de corrélation des formations miocènes du Sud de la dorsale tunisienne. *Note du Service Géologique de Tunisie* 38, 73–92.

Bismuth H. & Hooyberghs H.J.F. 1994: Foraminifères planctoniques et biostratigraphie de l'Oligocène et du Néogène dans le sondage de Korba-1 (Cap Bon, Tunisie nord orientale). *Bulletin des Centres de Recherches Exploration-Production Elf-Aquitaine* 18, 489–528.

Booth-Rea G., Gaidi S., Melki F., Marzougui W., Azañón J.M., Zargouni F., Galvé J.P. & Pérez-Peña J.V. 2018: Late Miocene Extensional Collapse of Northern Tunisia. *Tectonics* 37. https://doi.org/10.1029/2017TC004846

Bott M.H. P. 1959: The mechanism of oblique slip faulting. *Geological Magazine* 96, 109–117.

Boujamaoui M., Saadi M., Inoubli M.H., Zaghbib-Turki D. & Turki M.M. 2000: Géométrie des dépôts de la formation Beglia (Miocène moyen) et ses équivalents latéraux en Tunisie et dans le bloc pélagien: Sédimentologie et séquences de dépôts. *African Geoscience Review* 7, 55–73.

Buchanan J.G. & Buchanan P.G. 1995: Basin Inversion. *Journal of the Geological Society London, Special Publication* 88, 1–596.

Burollet P.F. & Ellouze N. 1986: L'évolution des bassins sédimentaires de la Tunisie centrale et orientale. *Bulletin Elf Aquitaine* 10, 49–68.

Chihi L., Galloul N. & Razgallah S. 2000: Paleoseismic events in Eastern Tunisia (Cap-Bon, Sahel) – seismites associated with Miocene–Pliocene and Quaternary sediments. *African Geoscience Review* 3, 307–314.

Colleuil B. 1976: Etude stratigraphique et néotectonique des formations néogènes et quaternaires de la région de Nabeul-Hammamet (Cap-Bon, Tunisie). *Diplôme d'Etudes Supérieures de Sciences Géologiques*, Nice, 1–94.

Cooper M.A., Williams G.D., de Graciansky P.C., Murphy R.W., Needham T., de Paor D., Stoneley R., Todd S.P., Turner J.P. & Ziegler P.A. 1989: Inversion tectonics – a discussion. In: Cooper M.A. & Williams G.D. (eds.): Inversion tectonics. *Geological Society, London, Special Publications* 44, 335–347.

Decrée S., Marignac C., Liégeois J.-P., Yans J., Ben Abdallah R. & Demaiffe D. 2014: Miocene magmatic evolution in the Nefza district (Northern Tunisia) and its relationship with the genesis of polymetallic mineralizations. *Lithos* 192–195, 240–258. https://doi.org/10.1016/j.lithos.2014.02.001

Demarcq G., Meon-Vilain H., Miguet R. & Kujawski H. 1976: Un bassin paralique néogène: celui de Skanès-Monastir (Tunisie orientale). *Notes Service Géologique de Tunisie* 42, 97–148.

Elmejdoub N. & Jedoui Y. 2009: Pleistocene raised marine deposits of the Cap Bon peninsula (N-E Tunisia): Records of sea-level highstands, climatic changes and coastal uplift. *Geomorphology* 112, 179–189. https://doi.org/10.1016/j.geomorph.2009.06.001

Fares J., Inoubli M.H., El Ouahichi A. & Hamouda F. 2006: Sequential and tectonic model approach of the Miocene series in the gulf of Hammamet (Northeastern Tunisia). *The 10th Tunisian Petroleum Exploration and Production conference*.

Frigui M., Ben Youssed M. & Ouaja M. 2016: Evidences of "Lago-Mare" episode around the Messinian-Pliocene boundary in eastern Tunisia (central Mediterranean). *Journal of African Earth Sciences* 123, 57–74.

Gaaloul N. & Razgallah S. 2008: Messinian palaeoenvironments in eastern Tunisia (Sahel and Gulf of Hammamet). *Geololgy, Ecology, Tropology* 32, 91–100.

Ghribi R. & Bouaziz S. 2010: Neotectonic evolution of the eastern Tunisian platform from paleostress reconstruction. *Journal of Hydrocarbons Mines and Environmental Research* 1, 14–25.

Ghribi R., Zaatra D. & Bouaziz S. 2018: Quaternary activity of the Monastir and Grombalia Fault systems in the North-Eastern Tunisia (Seismotectonic implication). *Geotectonics* 52, 100–113.

Glennie K.W. & Boegner P.L.E. 1981: Sole Pit inversion tectonics. In: Illing L.V. & Hobson G.D. (eds.): Petroleum Geology of the Continental Shelf of Northwest Europe. *Institute of Petroleum*, London, 110–120.

Grossi F., Gliozzi E. & Cosentino D. 2011: Paratethyan ostracod immigrants mark the biostratigraphy of the Messinian Salinity Crisis. *Joannea Geologie und Paläontologie* 11, 66–68.

Halloul N. & Gourgaud A. 2012: The post-collisional volcanism of northern Tunisia: Petrology and evolution through time. *Journal of African Earth Sciences* 63, 63–76.

Haq B.U., Hardenbol J. & Vail P.R. 1988: Mesozoic and Cenozoic chronostratigraphy and cycles of sea-level change. In: Wilgus C.K., Hastings B.S., Ross C.A., Posamentier H., Van Wagoner J. & Kendall C.G.S.C. (eds.): Sea Level Changes – An Integrated Approach. *SEPM Special Publication* 42, 71–108.

Hooyberghs H.J.F. 1987: Foraminifères planctoniques d'âge langhien (Miocène) dans la formation Aïn Grab au Cap Bon (Tunisie). *Note du Service Géologique de Tunisie* 55, 5–18.

Hooyberghs H.J.F. 1995: Synthèse sur la stratigraphie de l'Oligocène, Miocène et Pliocène de Tunisie. *Note du Service Géologique de Tunisie* 61, 63–72.

Hooyberghs H.J.F. & Ben Salem H. 1999: Biostratigraphie des foraminifères planctoniques de la formation Saouaf (Tortonien) dans le synclinal de Takelsa (Cap Bon, Tunisie). *Note du Service Géologique de Tunisie* 66, 113–124.

Kamoun Y., Hooyberghs H.J.F., Ben Youssef M., Zouari H. & Gaaloul N. 2001: Signature de la transgression du Messinien inférieur en Tunisie orientale. Coupe de l'oued Macera. *Note du Service Géologique de Tunisie* 68, 5–14.

Krijgsman W., Capella W., Simon, D., Hilgen F.J., Kouwenhoven T.J., Meijer P.T., Sierro F.J., Tulbure M.A., Berg B.C.J. van den Schee V. & Flecker R. 2018: The Gibraltar Corridor: Watergate of the Messinian Salinity Crisis. *Marine Geology* 403, 238–246. https://doi.org/10.1016/j.margeo.2018.06.008

Laaridhi-Ouazza N. & Bédir M. 2005: Les migrations tectono-magmatiques du Trias au Néogène sur la marge orientale de la Tunisie. *Africain Geosciences Revues* 11, 179–196.

Letouzey J. & Trimoliere P. 1980: Paleostress fields around the Mediterranean since the Mesozoic derived from microtectonics: comparisons with plate tectonic data. In Géologie des chaînes alpines issues de la Téthys. *Mémoires du Bureau de Recherches Géologiques et Minières* 115, 261–273.

Levander A., Bezada M.J., Niu F., Humphreys E.D., Palomeras I. & Thurner S.M. 2014: Subduction-driven recycling of continental margin lithosphere. *Nature* 515, 253–256.

Mahmoudi M. 1988: New proposal of stratigraphic subdivisions of the deposits attributed to the Tyrrhenian in Tunisia (Monastir region). *Bulletin de la Société Géologique de France* 8, 431–435.

Mannaï-Tayech B., Bobier C. & Méon H. 1992: Contribution à la connaissance de l'évolution des paléoenvironnements marginolittoraux néogènes du Cap Bon (Tunisie nord-orientale). Les oscillations climatiques observées sur la bordure occidentale du Détroit siculo-tunisien au Miocène et leurs rapports avec les fluctuations eustatiques. *8th International Palynological Congress*, Aix-en Provence, Abstracts.

Mascle G. & Mascle J. 2019: The Messinian salinity legacy: 50 years later. *Mediterranean Geoscience Reviews* 1, 5–15. https://doi.org/10.1007/s42990-019-0002-5

Mauz B., Elmejdoub N., Nathan R. & Jedoui Y. 2009: Last interglacial coastal environments in the Mediterranean–Saharan transition zone. *Palaeogeography, Palaeoclimatology, Palaeoecology* 279, 137–149. https://doi.org/10.1016/j.palaeo.2009.05.006

McClay K.R. & Buchanan P.G. 1992: Thrust faults in inverted extensional basins. In: Thrust Tectonics. *Springer*, Dordrecht, 93–104.

Mejri H., Balescu S., Lamothe M., Barre M., Abichou H. & Bouaziz S. 2012: Mise en évidence par la luminescence des feldspaths de deux hauts niveaux marins interglaciaires du Pléistocène moyen (MIS 7 et MIS 9) le long de la côte orientale de la Tunisie (Sahel). *Quaternaire* 23, 175–186.

Moissette P., Cornée J.J., Mannaï-Tayech B., Rabhi M., André J.P., Koskeridou E. & Méon H. 2010: The western edge of the Mediterranean Pelagian Platform: A Messinian mixed siliciclastic-carbonate ramp in northern Tunisia. *Palaeogeography, Palaeoclimatology, Palaeoecology* 285, 85–103. https://doi.org/10.1016/j.palaeo.2009.10.028

Morel J.C. 1989: Paleogeographic and tectonic evolution of Rif Belt (Morocco) from Tortonian to Present time. *Comptes Rendus Académiques en Sciences* 309, 2053–2059.

Ouahchi A., Hammouda F., Haddar Y. & Acheche M.H. 2002: Middle Miocene transtensional regime effect and impacts on the distribution of the Miocene petroleum systems in the northeastern offshore Tunisia. *Abstracts, Eight Tunisian petroleum exploration & production conference*, P85.

Rouvier H. 1977: Géologie de l'Extrême Nord tunisien. Tectoniques et paléogéographies superposées à l'extrémité orientale de la chaîne nord-maghrébine. *Thèse Doctorat en Sciences, Université Pierre et Marie Curie*, Paris, 1–703.

Salaj J. & Stranik Z. 1970: Contribution à l'étude stratigraphique du Miocène du synclinal de Saouaf (région du J. Fkirine, Tunisie orientale). *Notes du Service Géologique de Tunisie* 3, 79–82.

Sartori R., Carrara G., Torelli L. & Zitellini N. 2001: Neogene evolution of the southwestern Tyrrhenian Sea (Sardinia basin and western bathyal plain). *Marine Geology* 175, 47–66.

Sciuto F., Temani R. & Khayati H. 2020: Late Messinian ostracods from Eastern Tunisia. *Revue de Micropaléontologie* 71. https://doi.org/10.1016/j.revmic.2020.100467

Soumaya A., Ben Ayed N., Rajabi M., Meghraoui M., Delvaux D., Kadri A., Ziegler M., Maouche S. & Braham A. 2018: Active faulting geometry and stress pattern near complex strike-slip systems along the Maghreb region: Constraints on active convergence in the Western Mediterranean. *Tectonics* 37. https://doi.org/10.1029/2018TC004983

Turner J.P. & Williams C.A. 2004: Sedimentary basin inversion and intra-plate shortening, *Earth Sciences Revue* 65, 277–304. https://doi.org/10.1016/j.earscirev.2003.10.002

Van Hinsbergen D.J.J., Vissers R.L.M. & Spakman W. 2014: Origin and consequences of western Mediterranean subduction, rollback, and slab segmentation. *Tectonics* 33, 393–419. https://doi.org/10.1002/2013TC003349

Vissers R.L.M., Platt J.P., & Van der Wal D. 1995: Late orogenic extension of the Betic Cordillera and the Alboran Domain: A lithospheric view. *Tectonics* 14, 786–803.

Wallace R.E. 1951: Geometry of shearing stress and relation to faulting. *Journal of Geology* 59, 118–130.

Weijermars R., Roep T.B., Van den Eeckhout B., Postma G. & Kleverlaan K. 1985: Uplift history of a Betic fold nappe inferred from Neogene-Quaternary sedimentation and tectonics (in the Sierra Alhamilla and Almeria, Sorbas and Tabernas Basins of the Betic Cordilleras, SE Spain). *Geologie en Mijnbouw* 64, 397–411.

Zouaghi T., Bedir M., Melki F., Gabnti H., Gharsalli R., Bessioud A. & Zargouni F. 2011: Neogene sediment deformations and tectonic features in northeastern Tunisia: evidence for paleoseismicity. *Arabian Journal of Geosciences* 4, 1301–1314.